Effect of oxygen tension and rate of pressure reduction during decompression on central gas bubbles

R. E. REINERTSEN,[1] V. FLOOK,[2] S. KOTENG,[1] AND A. O. BRUBAKK[3]
[1]*Department of Extreme Work Environment, Stiftelsen for Industriell og Teknisk Forskning ved Norges Tekniske Høgskole (SINTEF) Unimed, N-7034 Trondheim, Norway;* [2]*SINTEF Unimed United Kingdom, Department of Biomedical Sciences, University of Aberdeen, Aberdeen AB91AS, United Kingdom; and* [3]*Department of Physiology and Biomedical Engineering, Norwegian University of Science and Technology, N-7005 Trondheim, Norway*

Reinertsen, R. E., V. Flook, S. Koteng, and A. O. Brubakk. Effect of oxygen tension and rate of pressure reduction during decompression on central gas bubbles. *J. Appl. Physiol.* 84(1): 351–356, 1998.—Reduction in ascent speed and an increase in the O_2 tension in the inspired air have been used to reduce the risk for decompression sickness. It has previously been reported that decompression speed and O_2 partial pressure are linearly related for human decompressions from saturation hyperbaric exposures. The constant of proportionality K (K = rate/partial pressure of inspired O_2) indicates the incidence of decompression sickness. The present study investigated the relationship among decompression rate, partial pressure of inspired O_2, and the number of central gas bubbles after a 3-h dive to 500 kPa while breathing nitrox with an O_2 content of 35 kPa. We used transesophageal ultrasonic scanning to determine the number of bubbles in the pulmonary artery of pigs. The results show that, for a given level of decompression stress, decompression rate and O_2 tension in the inspired air can be traded off against each other by using pulmonary artery bubbles as an end point. The results also seem to confirm that decompressions that have a high K value are more stressful.

saturation diving; venous gas emboli; swine; transesophageal echocardiographic transducer

DECOMPRESSION SICKNESS (DCS) may occur in any individual after a reduction in environmental pressure. Various procedures have been developed to reduce the risk for this. In addition to a reduction in ascent speed and the use of decompression stops, an increase in the O_2 tension in the inspired air has been used. This increase reduces the amount of inert gas and thus increases the gradient for inert gas elimination. Because it is generally held that gas bubbles in blood and tissue are the primary cause of DCS (1, 6), it is of interest to study the relationship among inspired O_2 tension, decompression rate, and intravascular gas-bubble formation.

It has been shown that, when decompressing from saturation, there is a linear relationship between the acceptable decompression rate and inspired O_2 partial pressure (PI_{O_2}) (10, 13), with DCS as the end point. Both theoretical models and examination of data from saturation dives lead to the relationship

$$K = \text{rate}/PI_{O_2} \quad (1)$$

described by Vann and Thalmann (12), where K is the constant of proportionality, rate is given as feet per hour (fph), and PI_{O_2} is given in atmospheres (atm). After examination of 579 human decompressions using heliox, Vann and Thalmann concluded that K = 10 fph/atm was the critical value dividing decompressions that led to DCS from those that did not. After the Atlantis III and Atlantis IV dives, Vann and Thalmann concluded that the safe value of K might decrease with increasing saturation depth (10). For helium-O_2 decompressions, safe K values range from 12 for saturation depths up to 100 feet of sea water (fsw) to 4 for saturation depths of 2,100–2,250 fsw. For nitrogen-O_2 dives, the values of K are lower, ranging from 5 to 3.5 for saturation depths from 40 to 190–200 fsw, respectively (10).

The present study was initiated to investigate the relationship among decompression rate, PI_{O_2}, and the amount of gas bubbles in the pulmonary artery after a 3-h dive to 500 kPa [40 m sea water (msw)] breathing nitrox with an O_2 content of 35 kPa. The experiments described here make use of transoesophageal ultrasonic scanning to determine the number of bubbles in the pulmonary artery of pigs. The relationship between pulmonary artery bubbles and the incidence of DCS has not been reliably determined; this is discussed by Nishi (9) in terms of Doppler detection of bubbles. However, it is of interest to determine the relationship between the value K (relating decompression rate to PI_{O_2}) and pulmonary artery bubble counts.

METHODS

Experimental animals. A total of 36 pigs (*Sus scrofa domestica* of the strain *Norsk landsvin*) were used. The pigs, both males and females, were 12 wk old, with body weights of 24.6 ± 1.4 kg. The animal experimentation was conducted in conformity with the *Guiding Principles for Research Involving Animals and Human Beings*. The experimental protocols were reviewed and approved by the Norwegian Committee for Animal Experiments.

Pressure profile and breathing gas. All animals were compressed to 500 kPa (40 msw) in 2 min while breathing nitrox (35 kPa O_2). They remained at this pressure for 3 h. The bottom time was followed by a linear decompression to the surface at a rate of 200, 100, or 67 kPa/h, giving a total decompression time of 2, 4, or 6 h. During decompression, the PI_{O_2} of the breathing gas was kept at 35, 100, or 200 kPa for the different experimental series. In the experiment with 200 kPa PO_2, the O_2 tension was kept at 100% from 10 msw to the surface, gradually reducing PI_{O_2} from 200 to 100 kPa. Pressure profiles for the experiments are shown in Fig. 1.

Surgical procedure. Before the experiments, the pigs were fasted for 16 h but with free access to water. At 20 min before induction of anesthesia, the pigs received premedication with azaperonum (Sedaperone, 7–9 mg/kg im; Janssen), and atro-

 0161-7567/98 $5.00 Copyright © 1998 the American Physiological Society

Downloaded from http://jap.physiology.org/ by 10.220.33.2 on November 18, 2017

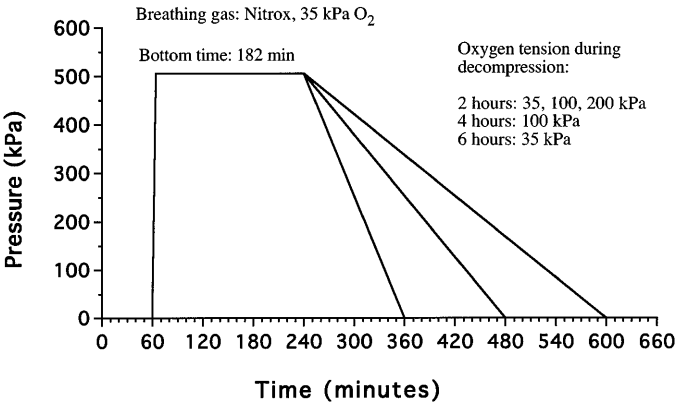

Fig. 1. Experimental pressure profiles. No. of experimental animals for each decompression (in kPa O_2/h): 8 pigs at 35/6, 100/2, and 100/4; 6 pigs at 200/2; and 5 pigs at 35/2. Detection of gas bubbles, measurements of blood gases, and calculations of constant of proportionality (K) values were done for all experimental series.

pinsulfate (Atropin, 1 mg iv; Hydro Pharma) was thereafter given via an ear vein. Anesthesia was induced by thiopental sodium (5 mg/kg Thiopenton; Natrium, Nycomed Pharma) and ketamine (20 mg/kg Ketalar; Parke, Davis). The anesthesia was maintained by a continuous iv infusion of ketamine in 0.9% NaCl (30 $mg \cdot kg^{-1} \cdot h^{-1}$) together with bolus doses of α-chloralose in 0.9% NaCl (10–15 mg/kg injected iv, 0.25% solution). A tracheotomy was performed to allow the pigs to breathe spontaneously through an endotracheal tube. Throughout the experiments, the pigs were in a supine posture. The depth of anesthesia was maintained at an even level, as judged by clinical observation of the various measured physiological variables.

Two polyethylene catheters were introduced into the left jugular vein and were moved into the pulmonary artery for measurement of pulmonary arterial pressure and to provide a means of obtaining mixed venous blood for gas analysis. A third catheter was positioned in the right atrium via the right jugular vein for measurements of central venous pressure. Furthermore, two catheters were inserted into the right femoral artery and advanced into the abdominal aorta for continuous monitoring of arterial pressure and to obtain blood samples for analysis of blood-gas composition. Blood hematocrit was measured at regular intervals throughout the experiment.

Deep body temperature was measured continuously throughout the experiments and was kept between 37.5 and 38.5°C through regulation of the chamber temperature.

Experimental setup and bubble detection. The experimental setup is shown in Fig. 2. Inside the chamber, the pig breathed via two bags, one containing inspiratory gas, the other expiratory gas. CO_2 and O_2 in the expired air (both mixed expired and end tidal) were measured together with respiratory frequency and flow (8). Blood gases were measured by using a Radiometer ABL 330. This instrument has been calibrated up to O_2 tensions of 300 kPa (14).

A transesophageal echocardiographic probe was inserted and positioned to obtain a simultaneous two-dimensional view of the pulmonary artery and the aorta (CFM 750; Vingmed Sound, Horten, Norway). It was assumed that the size distribution of the bubbles was the same. Because bubbles grow from nuclei that could be any uneven surface, the presence of catheters in the pulmonary artery may

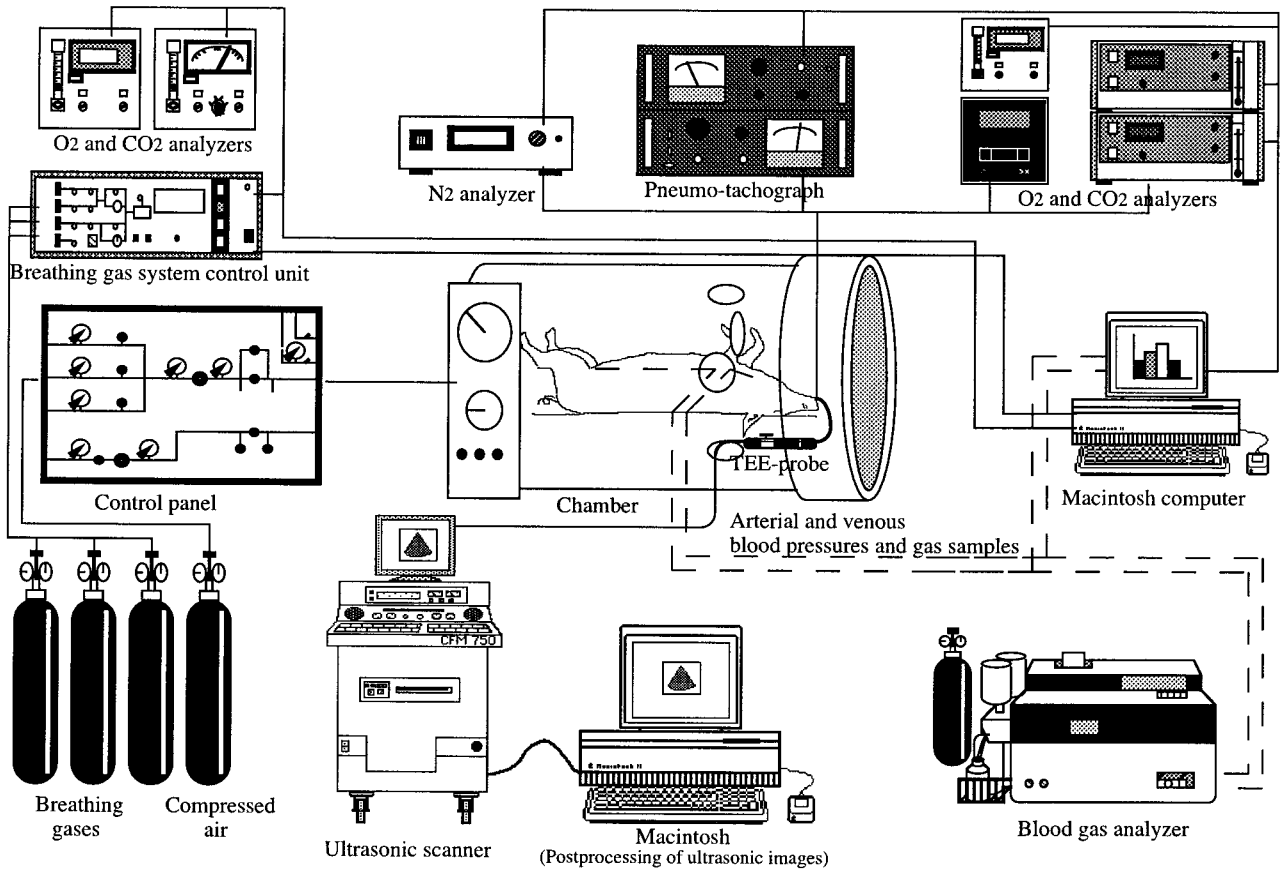

Fig. 2. Schematic figure of pressure chamber and its subsystems. TEE, transesophageal echocardiographic.

Downloaded from http://jap.physiology.org/ by 10.220.33.2 on November 18, 2017

increase the number of bubbles. However, this should not be a factor in this study, as catheters were used in all animals. Every 15th minute during decompression and for 90 min after surfacing (5-min intervals during the first 30 min after surfacing and 15-min intervals during the following 60 min), data were transferred to a Macintosh FxII computer. The data were analyzed by using a computer program for gas-bubble detection in the pulmonary artery and the aorta. The number of bubbles is given as number of bubbles per square centimeter (2). From the onset of the 1-h stabilization period, during the dive, and throughout a 90-min postdive period, the experiments were controlled by a preprogrammed computer (8). All measurements, apart from the blood-gas measurements and detection of gas bubbles, were recorded continuously by the computer. Predive data were collected during the 1-h period of stabilization.

Saturation level. The present study was designed to simulate saturation conditions. Exposure to maximum pressure was for 3 h. This bottom time is sufficient for producing 97% saturation as judged by the nitrogen content of the pulmonary artery blood (7). Saturation of some tissues (for example, fat or bone marrow) will require some additional time. Thus the slowest tissues may continue to take up gas during the early phase of decompression. This may be a source of extra bubbles for the slowest decompression, but there should be minimal effect on pulmonary artery bubbles, because the slowest tissues contribute only a very small percentage of gas to mixed venous blood.

Shunt fraction. The shunt fraction (i.e., the fraction of circulating blood that effectively bypasses the lungs) was calculated from the ratio of blood content of O_2 in arteries, pulmonary capillaries, and veins according to the formula

$$(Ca_{O_2} - Cc_{O_2})/(Cv_{O_2} - Cc_{O_2})$$

where C indicates blood content, a is arterial, v is venous, and c is end pulmonary capillary. Blood O_2 content is calculated from Po_2 by use of the pig oxyhemoglobin-dissociation curve (5). End pulmonary capillary Po_2 was assumed equal to alveolar partial pressure which was derived from end-tidal pressure of O_2.

Conversion factor for Vann's K value. Vann and Thalmann quote the *K* value (in fph/atm; see Ref. 12), relating the rate of ascent (in fph) to the Pi_{O_2} (in atm). A conversion factor of 0.030 is required when decompression is in kPa/h and O_2 pressure in kPa.

Statistical analysis of the data. Mean values ± SD are presented. The significance of differences between mean values was evaluated by Student's *t*-test. Linear correlations were fitted by the method of least squares. The limit of statistical significance was taken as $P < 0.05$.

RESULTS

Blood-gas levels. Table 1 gives arterial and venous O_2 and CO_2 partial pressures measured 30 min after the beginning of decompression. Both venous and arterial gases can be influenced by the presence of decompression bubbles through the effect of venous admixture. Therefore it is difficult to obtain measurements that relate only to a change in inspired gas unaffected by bubbles. By using the values at 30 min into decompression, we assume that there is a steady state after the change in inspired O_2. No bubbles were detected at this stage in any of the decompressions, no matter what the rate of pressure change. Whatever small, invisible bubbles may have been present, we assume that they had no influence on blood gases at that stage in the decompression. The blood-gas values reported in Table 1 are assumed to result only from the change in inspired O_2.

Table 1. *Partial pressure of blood gases and O_2 window for 5 experimental series 30 min after start of decompression*

	Pressure Profile, kPa O_2/h				
Blood Gas	35/2 (n=5)	35/6 (n=8)	100/2 (n=6)	100/4 (n=8)	200/2 (n=6)
Arterial O_2	24.1±5.5	22.5±5.0	59.2±15.0	49.4±14.8	97.6±28.7
Arterial CO_2	5.1±0.7	5.8±0.4	5.4±0.8	6.0±0.4	5.2±0.4
Venous O_2	6.7±0.6	7.5±0.9	7.9±0.6	9.6±1.6	12.1±2.9
Venous CO_2	5.9±0.4	6.5±0.6	6.1±0.9	7.2±0.3	6.4±0.6
O_2 window	21.8±0.9	14.7±1.2	86.0±1.3	82.7±1.7	180.4±3.2

Values are means ± SD in kPa. *n*, no. of animals (in parentheses). Pressure profile 100/2 consisted of 8 animals, but blood-gas values were measured in only 6 animals.

Table 1 also gives the values for the magnitude of the O_2 window derived from measurements taken at 30 min. During decompression, it is not possible to calculate the size of the O_2 window by assuming that inspired and venous nitrogen levels are identical. In addition to the fact that nitrogen is washing out of the body, arterial nitrogen levels are also influenced by the degree of shunt created by raised O_2 levels. This shunt also makes it impossible to use arterial blood gases to calculate the magnitude of the O_2 window. Therefore the O_2 window has been calculated by using the difference between the sum of O_2 plus CO_2 partial pressures in alveolar gas and venous blood. Values relate to BTPS conditions; therefore water vapor is constant to both.

Pulmonary artery bubble counts. The number of bubbles detected in the pulmonary artery is given as individual peak bubble count (Table 2) or maximum average bubble count for the group (Table 3). Furthermore, Fig. 3 shows average bubble counts against time for decompressions at 200 kPa/h using 100 kPa O_2, 200 kPa/h using 200 kPa O_2, 100 kPa/h using 100 kPa O_2,

Table 2. *Peak bubble count for each pig from decompressions at 67 kPa/h using 35 kPa O_2, 200 and 100 kPa/h using 100 kPa O_2, and 200 kPa/h using 200 kPa O_2*

Pressure Profile, kPa O_2/h			
35/6 (n=8)	100/2 (n=8)	100/4 (n=8)	200/2 (n=6)
15.7	13.0	1.1	0.5
4.2	3.7	5.6	0.3
1.2	15.9*	0.7	0.9
10.1	5.7	0.7	0.8
1.3	5.2	16.5	13.5*
5.3	8.2	5.3	1.0
15.8	3.7	0.2	
2.4	20.5*	0.6	

Value for peak bubble count is in no. of bubbles/cm^2; *n*, no. of animals. Value for bubble count is final bubble count. Values from pressure profile 35/2 are not included because all animals died before we could determine that bubbles had reached a peak. Individual final bubble counts from 5 animals from this series were 20.1, 21.2, 25.5, 15.7, and 21.0. *Animals that died before we could determine that the bubbles had reached a peak.

Downloaded from http://jap.physiology.org/ by 10.220.33.2 on November 18, 2017

Table 3. *Maximum average bubble count from decompressions as shown in Table 2*

Pressure Profile kPa O_2/h			
35/6 ($n = 8$)	100/2 ($n = 8$)	100/4 ($n = 8$)	200/2 ($n = 6$)
6.2 ± 5.5	6.5 ± 5.2	3.0 ± 4.3	2.6 ± 5.3

Values are means ± SD in no. of bubbles per cm^2; *n*, no. of animals. Final average bubble count for pressure profile 35/2 was 20.7 ± 3.5.

and 67 kPa/h using 35 kPa O_2. In the series in which all animals died before we could determine that the bubbles had reached a peak (decompression at 200 kPa/h using 35 kPa O_2), final bubble count has been used. The values for maximum average bubble count given in Table 3 are the maximum values of the average (Fig. 3). This differs from the average of peak bubble counts because different animals reached peak counts at different times. Maximum average bubble count is the value we have chosen to use when dealing with the average results from all pigs in a series. In the more detailed statistical analysis carried out using individual pigs, we have used each pig's own peak bubble count.

Effect of different inspired O_2 levels during decompression. Three different partial pressures of O_2 (35, 100, or 200 kPa) were studied at a decompression rate of 200 kPa/h. Changing the inspired O_2 from 35 to 100 to 200 kPa gave an average arterial O_2 tension over the decompression period of 24.1 ± 5.5, 59.2 ± 15.0, and 97.6 ± 28.7 kPa, respectively (Table 1). For the three series, blood-gas values were determined for five, six, and six pigs, respectively. As explained above, these blood-gas values are measured 30 min after the start of decompression. The results show that this pressure profile produced a significant number of bubbles detected in the pulmonary artery for each of the three different O_2 tensions. Venous bubbles were first detected ~1 h before surfacing, at a depth between 20 and 15 m, when the animals were breathing 35 kPa O_2 during decompression. With this level of inspired O_2, all pigs died within 15 min after surfacing, and one pig died 15 min before the surface was reached. Final average bubble count was 20.7 ± 3.5 bubbles/cm^2 (n = 5). Breathing gas with 100 kPa O_2 during the 2-h decompression resulted in a significant reduction in bubble formation (Table 2), and only two of the eight pigs died. The average bubble counts are shown in Fig. 3. Maximum average bubble count was 6.5 ± 5.2 bubbles/cm^2 (Table 3). When the O_2 tension of the gas breathed during decompression was increased to 200 kPa, bubble counts decreased further, and only one of the six pigs died (Table 2). Maximum average bubble count was 2.6 ± 5.3 bubbles/cm^2 (Table 3).

Effect of different rates of pressure reduction during decompression. To study the effect of decompression rate on bubble formation, we carried out two additional series of experiments in which decompression rates were decreased. Increasing the decompression time from 2 to 6 h, using 35 kPa O_2 during decompression, resulted in a significant reduction of venous gas-bubble numbers (Table 2). A 2-h decompression time for this gas composition resulted in a final average bubble count of 20.7 ± 3.5 bubbles/cm^2; increasing the decompression time to 6 h reduced the bubble count to a maximum average of 6.2 ± 5.5 bubbles/cm^2 (n = 8; Table 3).

The effect of decompression rate was also studied for the profile using nitrox with 100-kPa O_2 during decompression. When decompression time was increased from 2 to 4 h, maximum average bubble count decreased (not significantly) from 6.5 ± 5.2 to 3.0 ± 4.5 bubbles/cm^2 (n = 8; Table 3).

Relationship between decompression rate and inspired O_2 level. We have calculated the value K, as given in *Eq. 1*, for each of the decompressions. The results given in

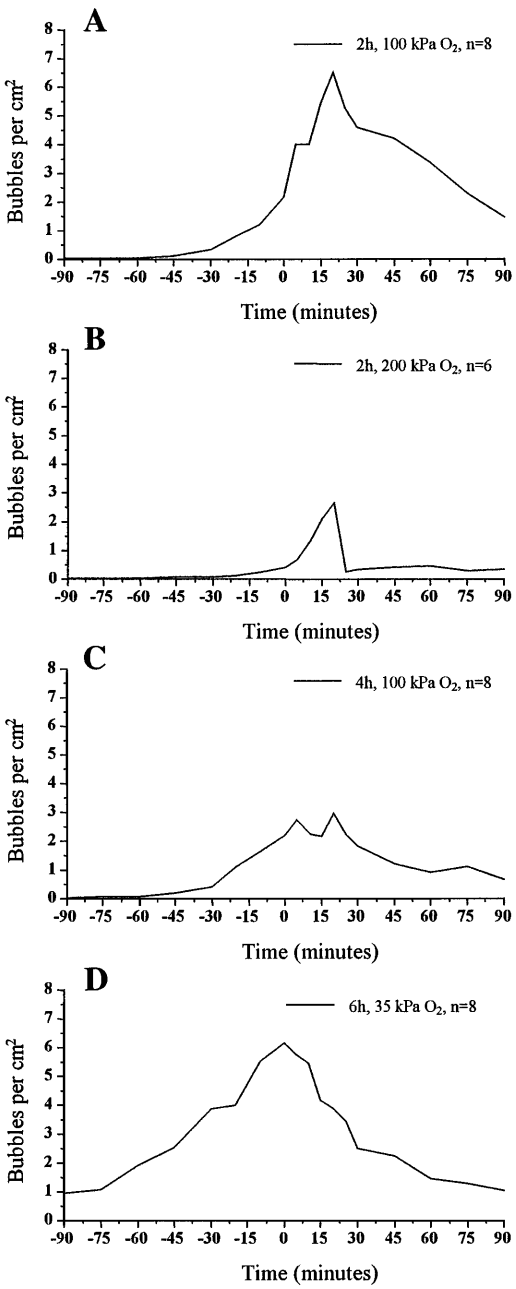

Fig. 3. Average bubble counts determined at each time of recording as a function of time for decompressions at 200 kPa/h using 100 kPa O_2 (*A*), 200 kPa/h using 200 kPa O_2 (*B*), 100 kPa/h using 100 kPa O_2 (*C*), and 67 kPa/h using 35 kPa O_2 (*D*). *Time 0*, time when surface is reached.

Downloaded from http://jap.physiology.org/ by 10.220.33.2 on November 18, 2017

Table 4. *K value relating decompression rate to P_{O_2}*

K Value	Pressure Profile, kPa O_2/h				
	35/2 ($n=5$)	35/6 ($n=8$)	100/2 ($n=8$)	100/4 ($n=8$)	200/2 ($n=6$)
K_I	5.7	1.9	2	1	1
K_a	8.3	3.0	4.1	2.0	2.1
K_w	9.2	4.5	2.3	1.2	1.1

Values are given per h; *n*, no. of animals; *K*, constant of proportionality for relationship between rate of ascent (kPa/h) and O_2 (in kPa) for all series of decompressions. K_I, inspired O_2 partial pressure; K_a, arterial O_2 partial pressure; and K_w, magnitude of the O_2 window.

Table 4 are designated K_I (*K* value for $P_{I_{O_2}}$). The highest K_I value, 5.7/h, corresponds to the profile that gave final average bubble count of 20.7 bubbles/cm^2. The two profiles that have K_I values of 1.9/h gave maximum average bubble counts of 6.2 and 6.5 bubbles/cm^2. The profiles with the lowest K_I value, 1/h, gave maximum average bubble counts of 3.0 and 2.6 bubbles/cm^2.

Relationship between decompression rate and arterial blood P_{O_2} (Pa_{O_2}). The vector by which $P_{I_{O_2}}$ can influence bubble production is arterial blood. We have therefore looked at the relationship between decompression rate and Pa_{O_2}. Values for the constant K_a, in the equation, Rate = $K_a \times Pa_{O_2}$, are given in Table 4. These values have been calculated by using the Pa_{O_2} as given in Table 1; that is, 30 min into the decompression.

Relationship between decompression rate and the magnitude of the O_2 window. The magnitude of the O_2 window determines the level of inert gas supersaturation that can exist without the possibility of bubble formation. We have therefore looked at the relationship between the magnitude of the O_2 window and decompression rate and determined the values of K_w derived from Rate = $K_w \times Pw_{O_2}$ where Pw_{O_2} is the O_2 window pressure. These are given in Table 4. The values have been calculated by using the O_2 window at 30 min into the decompression.

DISCUSSION

The original premise was that decompression speed and $P_{I_{O_2}}$ are linearly related for decompressions from saturation hyperbaric exposures, with the constant of proportionality *K* indicating the incidence of DCS. Thus all decompressions having the same value for *K* will have a similar incidence of DCS, and decompressions that have a higher *K* value should be more stressful. A comparison of the values for K_I in Table 4 and maximum average bubble count in Table 3 shows that there is a positive relationship between K_I values and the number of bubbles in the pulmonary artery. If we accept that there is a relationship between the incidence of DCS and the number of bubbles, these results confirm that decompressions that have a high *K* value are more stressful.

The arterial blood is, of course, the means by which changes in inspired O_2 are transmitted to the site of bubble production; therefore it might be expected that the formation of bubbles relates to the Pa_{O_2}. The magnitude of the O_2 window determines the threshold for inert gas supersaturation and therefore influences bubble formation. The results show that there is a linear relationship between both decompression speed and Pa_{O_2} as well as the magnitude of the O_2 window and decompression speed. For both K_a and K_w, similar values relate to decompressions that gave similar bubble counts. The value of *K* increases with increased bubble counts.

We have attempted to assess the relative importance of inspired O_2, arterial O_2, and the O_2 window. To do this, we have calculated the linear correlations coefficients for K_I, K_a, and K_w against bubbles by using, in this case, the peak bubble count for each animal. Figure

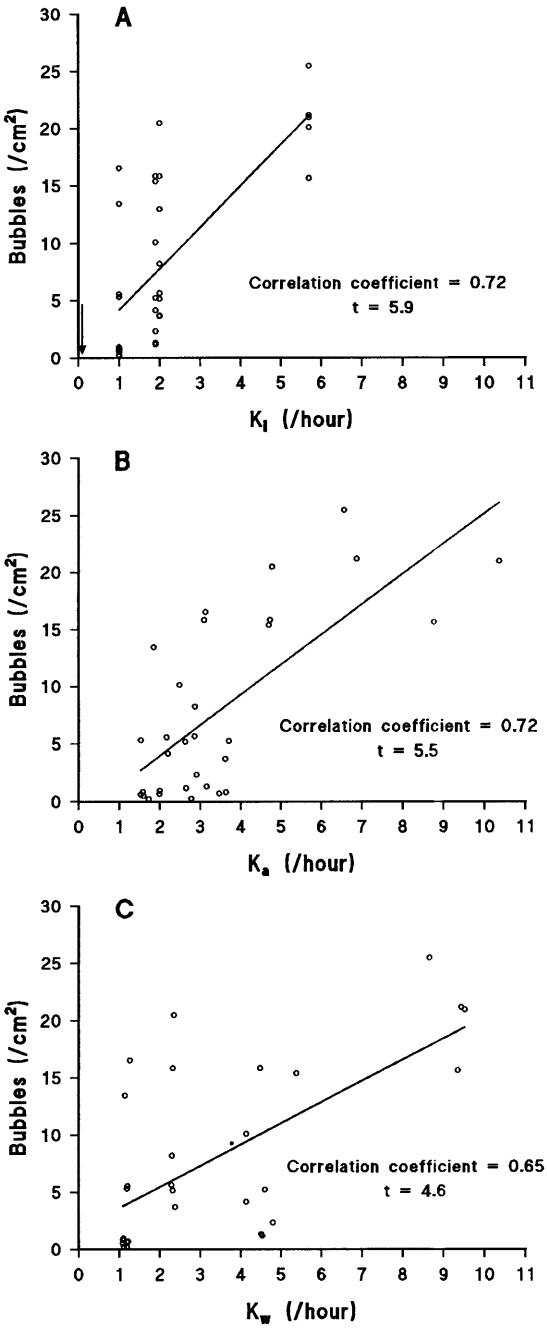

Fig. 4. Relationship between *K* values and bubble counts for inspired O_2 (K_I; *A*), arterial O_2 (K_a; *B*), O_2 window (K_w; *C*) and bubble nos. *A*: data for arrow pointing to *K* value 0.12 at bubble count of 0.3 bubbles/cm^2 are from Ref. 11.

Downloaded from http://jap.physiology.org/ by 10.220.33.2 on November 18, 2017

4 shows the relationship between K, the constant relating decompression rate and O_2, and bubble numbers. Figure 4*A* shows the relationship for inspired O_2. Figure 4, *B* and *C*, shows the relationship for arterial O_2 and the magnitude of the O_2 window. The equations of the lines relating K values and bubble numbers are

$$\text{Bubbles} = 3.43\ K_I + 0.71$$

$$\text{Bubbles} = 2.65\ K_a - 1.34$$

$$\text{Bubbles} = 1.86\ K_w + 1.75$$

The values for the correlation coefficients r and the t values for the linear correlation between the constants K_I, K_a, and K_w and bubble numbers are all significant at $P < 0.001$. The correlation coefficients rank in the order, from highest to lowest: arterial O_2, inspired O_2, and O_2 window. Both partial correlation and multiple regression analyses show that the relationship among the three is too close for the effect of any one to be significantly greater than that for either of the other two.

Although both Pa_{O_2} and the magnitude of the O_2 window depend on the PI_{O_2}, there are other factors that influence both. High PI_{O_2} causes an apparent increase in pulmonary shunt (4) that occurs to a varying degree between animals and that could alter the relationship between Pa_{O_2} and decompression rate. The magnitude of the O_2 window is dependent on both arterial and venous O_2 levels. Thus the relationship between decompression rate and O_2 window could be expected to be less close than for either of the other two.

Vann (11) suggested that decompression from any saturation depth resulted in the same incidence of DCS whatever the combination of decompression rate and PI_{O_2}, provided K was the same. He also showed that decompression from a given saturation depth resulted in a higher incidence of DCS as K increased. From data given in his paper, it is possible to calculate that, for decompression from 40 m, K ranging from 0.096 to 0.26/h will result in DCS incidence ranging from 2 to 60%. These K values are all considerably lower than those reported in this paper and reflect the very much slower decompression speeds used in Vann's work. Such low decompression rates are impractical for animal laboratory experiments. From Vann (11), a K value of 0.12/h would be expected to give a DCS incidence of 10% on decompression from saturation at 400 kPa. From work carried out as part of a separate study within our laboratory, we know that bubble counts in the region of 0.2–0.4 bubbles/cm^2 in human subjects correspond to a DCS incidence of ~7% (3). The arrow on Fig. 4*A* points to the K value 0.12/h at a bubble count of 0.3 bubbles/cm^2. This point fits well on the extrapolation of the line of best fit through our data. Thus, within the limits of our experimental variability and the accuracy of conversion from DCS to bubble counts for humans, we have shown that the relationship between decompression stress, as indicated by the number of pulmonary artery bubbles, and K_I is linear over a range extending from recorded levels in human trials to levels that are fatal in pigs. Linear relationships over a similarly wide range relate decompression stress and K_a and K_w. Our results show that, for a given level of decompression stress, decompression rate and O_2 tension in the inspired air can be traded off against each other by using pulmonary artery bubbles as an end point. These results may have significant implications for evaluation of decompression schedules.

We thank Øyvin Koteng, Arnfinn Sira, Anne Lise Ustad, and Olav Eftedal for their contribution to the experimental work.

This research was financed by Norsk Hydro, Statoil, Saga Petroleum, and the Norwegian Petroleum Directorate through the Forskning og Utvikling innen Dykketeknologi program.

Address for reprint requests: R. E. Reinertsen, Dept. of Extreme Work Environment, SINTEF Unimed, N-7034 Trondheim, Norway (E-mail: randi.reinertsen@unimed.sintef.no).

Received 16 September 1996; accepted in final form 18 September 1997.

REFERENCES

1. **Daniels, S.** The effect of pressure profile on bubble formation. In: *The Physiology of Diving. Proceedings of the 38th UHMS Workshop*, edited by R. D. Vann. Bethesda, MD: Undersea and Hyperbaric Medical Society, 1987, p. 107–208.
2. **Eftedal, O., and A. O. Brubakk.** Detecting intravascular gas bubbles in ultrasonic images. *Med. Biol. Eng. Comput.* 31: 627–633, 1993.
3. **Eftedal, O., and A. O. Brubakk.** Observed bubbles and decompression illness incidence. *Undersea Hyperbaric Med.* 23, *Suppl.*: S65–S66, 1996.
4. **Flook, V., S. Koteng, I. Holmen, and A. O. Brubakk.** The effect of decompression on pulmonary dead space. In: *Proceedings of the 20th Annual Meeting of EUBS*, edited by M. Cimsit. Istanbul, Turkey: European Undersea Biomedical Society, 1994, p. 271–276.
5. **Gomez, D. M.** Considerations of oxygen hemoglobin equilibrium in the physiological state. *Am. J. Physiol.* 200: 135–142, 1961.
6. **Hallenbeck, J. M., and J. C. Andersen.** Pathogenesis of the decompression disorders. In: *The Physiology and Medicine of Diving*, edited by P. B. Bennett and D. H. Elliott. San Pedro, CA: Best, 1982, p. 435–460.
7. **Holmen, I. M., V. Flook, and A. O. Brubakk.** Uptake and washout curves for nitrogen in pigs. In: *Proceedings of the 19th Annual Meeting of EUBS*, edited by R. E. Reinertsen, A. O. Brubakk and G. Bolstad. Trondheim, Norway: European Undersea Biomedical Society, 1993, p. 78–83.
8. **Kleven, A., A. Sira, and A. O. Brubakk.** Chamber guard: automatic control and data acquisition system for pressure chambers. In: *Proceedings of the XVII Annual Meeting of EUBS, Crete*, edited by N. S. Trikilis. Trondheim, Norway: European Undersea Biomedical Society, 1991, p. 317–324.
9. **Nishi, R. Y.** Doppler and ultrasonic bubble detection. In: *The Physiology and Medicine of Diving*, edited by P. B. Bennett and D. H. Elliott. London: Saunders, 1993, p. 433–453.
10. **Vann, R. D.** *Decompression Mechanics and Decompression Schedule Calculations.* Washington, DC: US Dept. of Navy, 1984. (Office of Naval Research Contract N-00014–83-K-0019 Final Report)
11. **Vann, R. D.** Saturation decompression with nitrogen-oxygen. In: *Proceedings of the 8th Meeting of the United States-Japan Cooperative Program in Natural Resources Panel of Diving Physiology and Technology. Washington, DC 6–17 June 1985.* Washington, DC: US Dept. of Commerce, 1986, p. 77–102.
12. **Vann, R. D., and E. D. Thalmann.** Decompression physiology and practice. In: *The Physiology and Medicine of Diving*, edited by P. B. Bennett and D. H. Elliott. London: Saunders, 1993, p. 376–432.
13. **Vorosmarti, J., E. E. P. Barnard, J. Williams, and R. de G. Hanson.** Nitrogen elimination in man during steady-state hyperbaric exposures. *Undersea Biomed. Res.* 5: 243–252, 1978.
14. **Weaver, L. K., S. Howe, and S. L. Berlin.** Monobaric measurements of O_2 tension and saline tonometered under hyperbaric conditions. *J. Hyperbaric Med.* 5: 29–38, 1990.

Downloaded from http://jap.physiology.org/ by 10.220.33.2 on November 18, 2017